

See discussions, stats, and author profiles for this publication at: <https://www.researchgate.net/publication/231681486>

Light Propagation in Composite Two-Dimensional Arrays of Polystyrene Spherical Particles

ARTICLE *in* LANGMUIR · OCTOBER 1999

Impact Factor: 4.46 · DOI: 10.1021/la990676b

CITATIONS

34

READS

24

6 AUTHORS, INCLUDING:



Tetsuya Miwa

Japan Agency for Marine-Earth Science Tech...

52 PUBLICATIONS 1,188 CITATIONS

SEE PROFILE



Donald A. Tryk

University of Yamanashi

250 PUBLICATIONS 15,560 CITATIONS

SEE PROFILE

Light Propagation in Composite Two-Dimensional Arrays of Polystyrene Spherical Particles

Sachiko I. Matsushita,[†] Yoshie Yagi,[†] Tetsuya Miwa,[‡] Donald A. Tryk,[†]
Takao Koda,[§] and Akira Fujishima^{*,†}

Department of Applied Chemistry, School of Engineering, The University of Tokyo,
7-3-1 Hongo, Bunkyo-ku, Tokyo 113-8656, Japan, Frontier Research Program for Deep-Sea
Extremophiles, Japan Marine Sciences & Technology Center, 2-15 Natsushima-cho,
Yokosuka 237-0061, Japan, and Department of Mathematical and Physical Science, Faculty of
Science, Japan Women's University, 2-8-1 Mejirodai, Bunkyo-ku, Tokyo 112-8681, Japan

Received June 1, 1999. In Final Form: August 25, 1999

Light propagation in composite two-dimensional spherical arrays in which mixtures of fluorescent and nonfluorescent polystyrene latex particles (3, 1, 0.5 μm) are packed in a highly dense, highly oriented manner on a solid surface was observed by use of fluorescence microscopy and phase-contrast microscopy. In addition, by means of through-focusing, we were able to determine directly the stacking mode, e.g., face-centered-cubic packing or hexagonal close packing, in up to three layers. The propagation modes can be divided into two types: one inside the particles and the other on the particle surfaces. The contribution of these two modes appears to be dependent upon the relative light frequency.

Introduction

Two-dimensionally (2D) ordered arrays, in which fine particles or protein molecules are densely packed in a highly oriented fashion, have been extensively studied as new types of nanoscale architecture.¹ The mechanism of formation for such 2D arrays has been discussed in the literature from the viewpoint of high-density optical storage media² and that of the orientation of protein molecules.^{3,4} Recently, a new viewpoint of 2D array research has arisen from the field of physics, that is, the 2D array as a photonic devices^{5,6} especially as a photonic crystal.⁷ Photonic crystals, in which photons behave the same way as electrons do in semiconductors,^{8,9} are periodic dielectric crystals.^{10–14} Two-dimensional arrays also have the same periodic dielectric structures,^{15,16} i.e., periodic structures of solid spheres and air (the same as three-

dimensional colloidal crystals),^{17–19} and thus it is expected that 2D arrays may function as quasi-2D photonic-type crystals (the prefix “quasi-” being used to indicate that the array does not have an infinite number of parallel mirror planes, as an array of cylindrical posts would, and is thus not a true 2D array).^{20–23}

When we first considered the 2D array for the study of photonic devices, we were interested in precisely how the photons propagate in the array. To examine the propagation in detail, we attempted to put the light source directly in the 2D array.²⁴ It is straightforward to make such an array if one uses the general 2D array preparation method, which makes use of lateral capillary forces between colloidal particles,²⁵ with one modification: the colloidal suspension contains two different types of particles, nonfluorescent polystyrene (PSt) together with fluorescent PSt particles.²⁴ The fluorescent particles were expected to function as light sources in the 2D array.^{26,27} In this paper, we describe how the photons propagate in this 2D array, within both single layers and triple layers. In addition, we also show the stacking mode information in triple layers using this light propagation. These informa-

[†] The University of Tokyo.

[‡] Japan Marine Sciences & Technology Center.

[§] Japan Women's University.

(1) Denkov, N. D.; Velev, O. D.; Kralchevsky, P. A.; Ivaonov, I. B.; Yoshimura, H.; Nagayama, K. *Nature* **1993**, *361*, 26.

(2) Micheletto, R.; Fukuda, H.; Ohtsu, M. *Langmuir* **1995**, *11*, 3333.

(3) Nagayama, K.; Takeda, S.; Endo, S.; Yoshimura, H. *Jpn. J. Appl. Phys.* **1995**, *34*, 3947.

(4) Velikov, K. P.; Durst, F.; Velev, O. D. *Langmuir* **1998**, *14*, 1148.

(5) Velev, O. D.; Jede, T. A.; Lobo, R. F.; Lenhoff, A. M. *Chem. Mater.* **1998**, *10*, 3597.

(6) Matsushita, S.; Miwa, T.; Fujishima, A. *Chem. Lett.* **1997**, *309*, 925.

(7) Miyazaki, H.; Ohtaka, K. *Phys. Rev. B* **1998**, *58* (11), 6920.

(8) Taubes, G. *Science* **1997**, *278*, 1709.

(9) Joannopoulos, J. D.; Meade, R. D.; Winn, J. N. *Photonic Crystals*; Princeton University Press: New Jersey, 1995.

(10) Wijnhoven, J. E. G. J.; Vos, W. L. *Science* **1998**, *281*, 802.

(11) Zakhidov, A. A.; Baughman, R. H.; Iqbal, Z.; Cui, C.; Khayrullin, I.; Dantas, S. O.; Marti, J.; Ralchenko, V. G. *Science* **1998**, *282*, 897.

(12) Ho, K. M.; Chan, C. T.; Soukoulis, C. M. *Phys. Rev. Lett.* **1990**, *65*, 3152.

(13) Villeneuve, P. R.; Piche, M. *Prog. Quantum Electron.* **1994**, *18*, 153.

(14) Yablonovitch, E. *J. Opt. Soc. Am. B* **1993**, *10*, 283.

(15) Fukuda, K.; Sun, H.; Matsuo, S.; Misawa, H. *Jpn. J. Appl. Phys.* **1998**, *37*, L508.

(16) Matsushita, S. I.; Miwa, T.; Tryk, D. A.; Fujishima, A. *Langmuir* **1998**, *14*, 6441.

(17) Miguez, H.; Blanco, A.; Meseguer, F.; Lopez, C.; Yates, H. M.; Pemble, M. E.; Fornes, V.; Mifsud, A. *Phys. Rev. B* **1999**, *59*, 1563.

(18) Bogomolov, V. N.; Gaponenko, S. V.; Germanenko, I. N.; Kapitonov, A. M.; Petrov, E. P.; Gaponenko, N. V.; Prokofiev, A. V.; Ponyavina, A. N.; Silvanovich, N. I.; Samoilovich, S. M. *Phys. Rev. E* **1997**, *55*, 7619.

(19) Brown, E. R.; McMahon, O. B. *Appl. Phys. Lett.* **1995**, *67*, 2138.

(20) Matsushita, S.; Minami, F.; Imada, A.; Shimada, R.; Koda, T. *Superlattices Microstruct.* **1999**, *25* (1–2), 347.

(21) Yamasaki, T.; Tsutsui, T. *Appl. Phys. Lett.* **1998**, *72*, 1957.

(22) Fujimura, T.; Itoh, T.; Hayashibe, K.; Edamatsu, K.; Shimoyama, K.; Shimada, R.; Imada, A.; Koda, T.; Segawa, Y.; Chiba, N.; Muramatsu, H.; Ataka, T. *Mater. Sci. Eng. B* **1997**, *B48*, 94.

(23) Fujimura, T.; Edamatsu, K.; Itoh, T.; Shimada, R.; Imada, A.; Koda, T.; Chiba, N.; Muramatsu, H.; Ataka, T. *Opt. Lett.* **1997**, *22*, 489.

(24) Matsushita, S.; Miwa, T.; Fujishima, A. *Langmuir* **1997**, *13*, 2582.

(25) Kralchevsky, P. A.; Nagayama, K. *Langmuir* **1994**, *10*, 23.

(26) Petrov, E. B.; Bogomolov, V. N.; Kalosha, I. I.; Gaponenko, S. V. *Phys. Rev. Lett.* **1998**, *81*, 77.

(27) Romanov, S. G.; Fokin, A. V.; Alperovich, V. I.; Johnson, N. P.; De La Rue, R. M. *Phys. Stat. Sol. A* **1997**, *164*, 169.

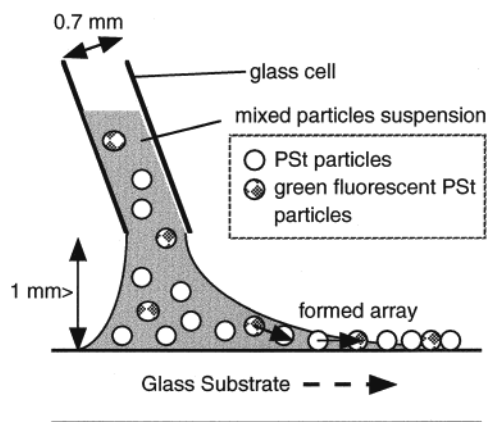


Figure 1. Schematic diagram of the fabrication of the composite 2D arrays. The height of the meniscus is one important parameter to control the number of the layers. Therefore, the height of the cell can be controlled using a *z*-axis motor. During preparation of the array, the substrate is translated horizontally using a *x*-axis motor.

tion would be quite useful for the study of 2D array, not only for the application but also for basic research for colloids.

Materials and Methods

The 2D array single and triple layers were prepared from water suspensions of commercial nonfluorescent monodisperse ($3.06 \pm 0.08 \mu\text{m}$, $0.930 \pm 0.013 \mu\text{m}$, $0.519 \pm 0.007 \mu\text{m}$) polystyrene microparticles (Polybead microspheres, Polysciences, Inc.). Green fluorescent particles ($\lambda_{\text{ex}}/\lambda_{\text{em}}$ 458/540 nm) of essentially the same dimensions ($3.00 \pm 0.08 \mu\text{m}$, $1.03 \pm 0.02 \mu\text{m}$, $0.499 \pm 0.007 \mu\text{m}$ diameter; Fluoresbrite microspheres, Polysciences, Inc.) were mixed with the nonfluorescent particles such that the fluorescent particles were present at relatively low fractions, either 1:32, 1:400, or 1:1200 (green nonfluorescent).

Approximately 0.5 mL of the mixed suspension was used for the array fabrication. The technique for the preparation of 2D arrays originally proposed by Nagayama et al. makes use of water evaporation and lateral capillary forces²⁸ to control the number of layers (Figure 1).^{24,29} The substrates were nonfluorescent glass slides (Micro-Slide glass, Matsunami Co., Japan). To establish the optimum experimental conditions, the direct visual observation during the particle assembly process, made possible by the use of an optical microscope equipped with a CCD camera, was found to be quite advantageous.

Well-ordered 2D arrays formed in this fashion, with a typical area of $18 \text{ mm} \times 25 \text{ mm}$, were illuminated by means of an Hg–Xe lamp, with the appropriate suitable excitation light passed through the lens of the fluorescence microscope (BX60-34-FLBD1, Olympus). We used an excitation filter (BP460-490, Olympus) which allows light of wavelengths from 460 to 490 nm to pass. The absorption filter (BA515F, Olympus) allows light of wavelengths greater than 515 nm to pass; i.e., the fluorescence emission from the sample can be detected. We used a combination of phase-contrast microscopy and fluorescence microscopy. Both techniques were available in the same microscope, so that we were easily able to observe the same area to obtain information on both packing and light propagation.

Results and Discussion

The mixed suspensions of fine particles were found to be stable, i.e., no flocculation, and we were able to prepare composite 2D arrays on the substrate. Even with two or three different types of particles, the composite 2D arrays exhibited high density, highly oriented hexagonal packing for each of the three diameters, i.e., $3 \mu\text{m}$ (Figure 2a), $1 \mu\text{m}$

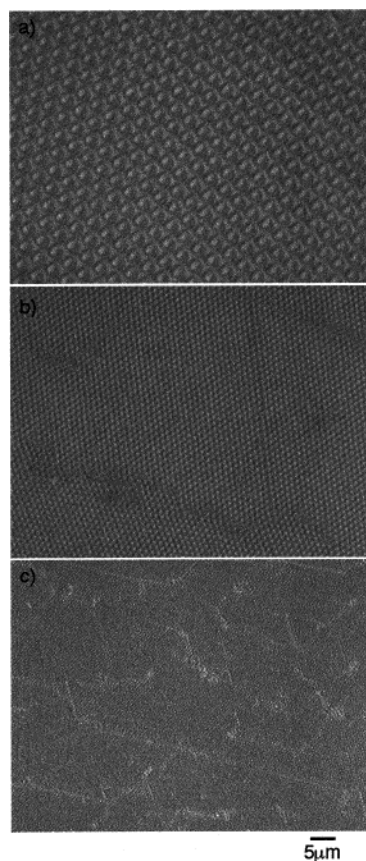


Figure 2. Phase-contrast microscopic images of single layers of the composite 2D arrays of (a) 3 (b) 1 and (c) $0.5 \mu\text{m}$ diameter particles.

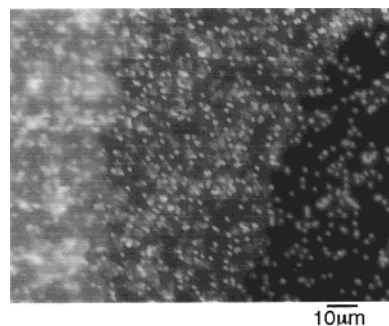


Figure 3. Typical fluorescent microscopic image of the edge of a triple layer of a composite green-fluorescing 2D array, showing the single, double, and triple layers.

μm (Figure 2b), and $0.5 \mu\text{m}$ (Figure 2c). This result showed that the size difference and any possible difference in surface properties between the nonfluorescent and fluorescent PSt particles were small enough that an array was able to form.²⁴ Although these arrays are composed of many polycrystalline domains, which can be seen in Figure 2c, the sizes of the domains were large enough to observe the light propagation in each domain, as discussed below.

At the edge of a triple layer, the single, double, and triple layers can be observed going from left to right in Figure 3 for an array of $1 \mu\text{m}$ particles (1:32 ratio). The light emitted from the triple layer is greatest due to the accumulation of fluorescence from particles in the three layers. Therefore, during the observation, we controlled the power of the excitation light for proper observation, depending not only on the number of the layers but also on the particle diameter. For example, a $3 \mu\text{m}$ fluorescent

(28) Denkov, N. D.; Velev, O. D.; Kralchevsky, P. A.; Ivanov, I. B.; Yoshimura, H.; Nagayama, K. *Langmuir* **1992**, *8*, 3183.

(29) Dimitrov, A. S.; Nagayama, K. *Langmuir* **1996**, *12*, 1303.

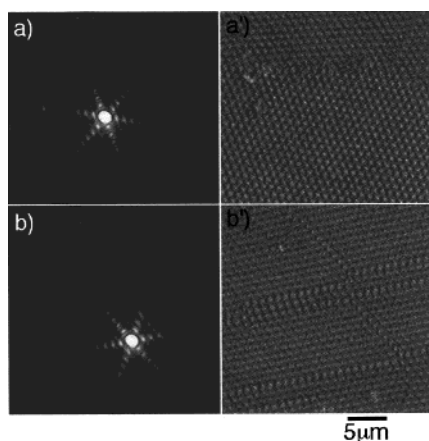


Figure 4. Light propagation in single layers of monodisperse polystyrene particles consisting of a mixture of green-fluorescing and nonfluorescent particles (all particles are $1\ \mu\text{m}$ diameter.). (a' and b') Phase-contrast microscopic images of each image.

particle emits much more light than does a $0.5\ \mu\text{m}$ particle. However, as shown below, the power of the emitted light had almost no effect on the type of light propagation.

Anisotropic Light Propagation in the Single Layer. Fluorescence microscopic images of a close-packed single layer containing green fluorescent particles in a composite 2D array ($1\ \mu\text{m}$ diameter, 1:32 ratio) are shown in Figure 4. In addition to the bright fluorescence emitted from a green-fluorescing particle, emission is also observed at additional nearby spots in 6-fold symmetrical patterns (Figure 4a,b).²³ Comparing these images with the phase-contrast optical microscopic images of the same area (Figure 4a' and 4b', respectively), we find that the emitted light does not locate at the fluorescent particles but can propagate along rows of adjoining nonfluorescent close-packed spheres.

This relationship between the type of light propagation and the crystal packing of the particles is best when the packing is close to ideal; i.e., adjoining particles are essentially touching. Nonidealities in light propagation can be observed at defects. For example, in Figure 4a, at the end of the ray emanating horizontally to the left, a dot of stronger light intensity is observed. From the phase-contrast-microscopic image, we find that this dot is at a point defect in the array (Figure 4a'). Moreover, at the edges of the domains, the light propagation is completely stopped, as found at the right side of the pattern in Figure 4b,b'. These phenomena are understandable in terms of the difference in the refractive indices of polystyrene ($n = 1.46$) and air ($n = 1.00$), as discussed later.^{30,31}

Size-Dependent Propagation in the Single Layer. This straight-line-propagation mode is more clearly observed in the composite 2D array of the $3\ \mu\text{m}$ diameter particles (Figure 5a). Again, we can observe 6-fold symmetric patterns, but as already mentioned, there is more light emitted than that from the $1\ \mu\text{m}$ diameter particles (Figure 5b), and the light emanating directly from the fluorescent particle is observed as a bright hexagon. A schematic model for the straight-line-type propagation observed in Figure 5a is shown in Figure 5c. This straight-line-type propagation can be subdivided into three parts: (1) the light emitted from the fluorescent particle propagates through the surrounding air and, in

the case of the $3\ \mu\text{m}$ particle array, is reflected off the walls of the adjoining nonfluorescent particles, behavior that is different from that observed with smaller particles (discussed later); (2) the emitted light propagates within the bulk of the particle and between particles at the point of contact; and (3) the light impinging on a particle that has propagated through the air from an adjoining particle is scattered from the surface, creating a crescent shape. Of course, as an additional propagation mode, we can also consider the light which passes through the glass substrate ($n \sim 1.5$) and is thus observed in the spaces between particles. However, in the present paper, we will not discuss this substrate-related mode.

The contribution of the straight-line-propagation mode changes with the particle diameter. As the particle diameter decreases, this contribution also decreases. The propagation pattern of green light ($\lambda_{\text{em}} = 540\ \text{nm}$) in the $500\ \text{nm}$ diameter particle array is shown in Figure 6a. The observed patterns became fuzzy, since the particle size is nearly the diffraction limit for the focus of the microscope; however, they were enough clear to observe the tendency of the pattern. For type 1 propagation, the light emitted from the fluorescent particle no longer reflects off the adjoining particles; instead, there is dispersion of the light due to diffraction, and the result is a vague illuminated polygon that appears to include the six nonfluorescent particles adjoining the fluorescent particle. Type 2 propagation, the main mode for straight-line propagation, is not observed to a significant extent, and thus type 3 propagation, which is closely associated with type 2, is also not observed. These results are understandable because the particle diameter is approximately the same as the wavelength of the propagated light.

Another type of propagation in the array can be suggested, which we will designate type 4 (Figure 6b). On the surfaces of the illuminated PSt particles, there are evanescent waves, which generally cannot be observed. However, because of the small space between the $500\ \text{nm}$ diameter particles, the evanescent waves are scattered on the surfaces of the adjoining particles, i.e., the latter act as probes, and the scattered light can be observed.

From the results presented thus far, we propose that when the particle diameter (D) is sufficiently large ($D > 2\lambda$), we can observe the straight-line-propagation mode but not the evanescent wave scattering mode, because the space between particles is too large. When the particle diameter is sufficiently small ($D \leq \lambda$), we can observe the scattered light arising from the evanescent wave but not straight-line propagation, because the light cannot propagate within the particles. These propagation types will be discussed in more detail in connection with the triple layers.

Light Propagation in the Triple Layer. If 2D arrays are to be used for the study of photonic crystals, we should determine where the domains are, what their sizes are, and whether the packing is cubic close-packed (ccp) or hexagonal close-packed (hcp). However, although van Blaaderen et al. had already reported some of the stacking information in colloidal crystals using confocal microscopy,³² these types of information have not been discussed before in terms of 2D array studies. In this section, we would like to show the information that can be obtained from the light propagation patterns in triple layers with well-defined packing structures, and also to show the particle size dependence of the vertical propagation patterns.

(30) Dushkin, C. D.; Nagayama, K.; Miwa, T.; Kralchevsky, P. A. *Langmuir* **1993**, *9*, 3695.

(31) Yagi, Y.; Matsushita, S. I.; Tryk, D. A.; Koda, T.; Fujishima, A. *Langmuir*, in press.

(32) van Blaaderen, A.; Ruel, R.; Wiltzius, P. *Nature* **1997**, *385*, 321.

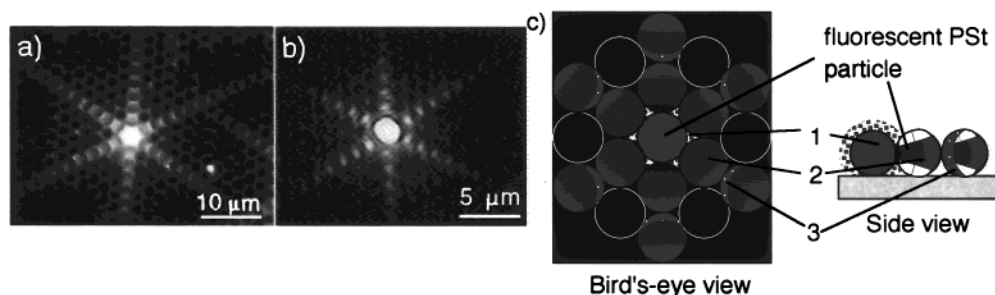


Figure 5. Size-dependent light propagation in single layers of monodisperse polystyrene particles consisting of a mixture of green-fluorescing particles; the particle diameter is (a) 3 and (b) 1 μm . Schematic diagrams for the three types of light propagation are shown in (c). This straight line-type propagation can be subdivided into three parts: (1) the light emitted from the fluorescent particle propagates through the surrounding air; (2) the emitted light propagates within the bulk of the particle and between particles at the point of contact; (3) the light impinging on a particle that has propagated through the air from an adjoining particle is scattered from the surface, creating a crescent shape.

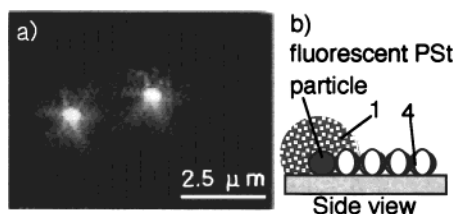


Figure 6. Size-dependent light propagation in single layers of monodisperse polystyrene particles consisting of a mixture of green-fluorescing particles; the particle diameter is 0.5 μm . Schematic diagrams for the two types of light propagation are shown in (b). On the surfaces of the illuminated PST particles, there are evanescent waves, which generally cannot be observed. However, because of the small space between the 500 nm diameter particles, the evanescent waves are scattered on the surfaces of the adjoining particles; i.e., the latter act as probes, and the scattered light can be observed. We named this propagation "type 4".

Figure 7a shows a fluorescence microscopic image observed for a triple layer of 1 μm diameter particles (1:1200). The observed patterns are classified into several types: (I) when the fluorescent particle is located in the top (third) layer, the top view shows only a single bright spot centered on the fluorescent particle; (II) when the fluorescent particle is located in the middle (second) layer, a triangular pattern is observed when the focal plane is in the top layer; and (III) particularly interesting patterns are observed when the fluorescent particle is in the bottom layer, i.e., triangular arrays composed of six dots and hexagonal arrays composed of seven dots. By means of through-focusing with the fluorescence microscope (to be discussed in detail later), we have confirmed that the hexagonal arrays correspond to emission from hcp packing regions, while the triangular arrays correspond to emission from fcc packing regions. In the phase-contrast optical microscopic image (Figure 7b), domains can be observed; comparing this image with the fluorescence image of the triple layer (Figure 7a), we can see that only a single type of pattern exists within a single domain.

Figures 8 and 9 show a series of detailed through-focus images for fcc domains and hcp domains, respectively, for arrays made up of 3 μm particles, 1 μm particles, and 0.5 μm particles, respectively.

Let us explain the light propagation in the 3 μm particle array at first. As the focal plane is raised, the observed patterns exhibit the following changes: in the bottom layer, the fluorescing particles show up as fuzzy circles (Figures 8a, 9a). When the focal plane is raised to the second layer, triangular arrays of three bright spots, which are those that are in direct contact with the fluorescent particle in the first layer, and are thus illuminated

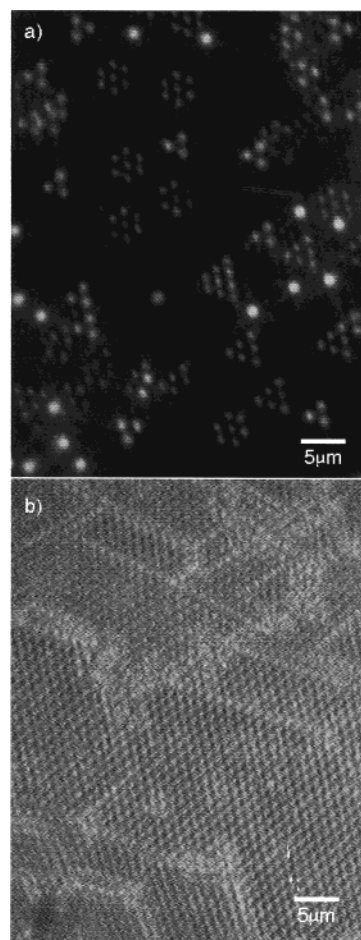


Figure 7. Light propagation in a triple layer of monodisperse polystyrene particles (1 μm diameter) consisting of a mixture of green-fluorescing and nonfluorescing particles (1:1200). The phase-contrast-microscopic image of (a) is also shown in (b).

efficiently by it, can be observed in both types of domains (Figures 8b, 9b). These are in direct contact with the fluorescing particles in the bottom layer, and this propagation type is exactly type 2, which we discussed above.

The illuminated patterns differ for fcc and hcp domains when the focal plane is raised to the top (third) layer. In the fcc domain, the pattern observed when the focal plane is at the bottom edge of the top layer is a triangle, each vertex being composed of three small hat-shaped patterns (Figure 8c). The large round portion of each hat arises due to type 2 light propagation, and the two small brim-shaped portions of each hat are caused by the diffraction

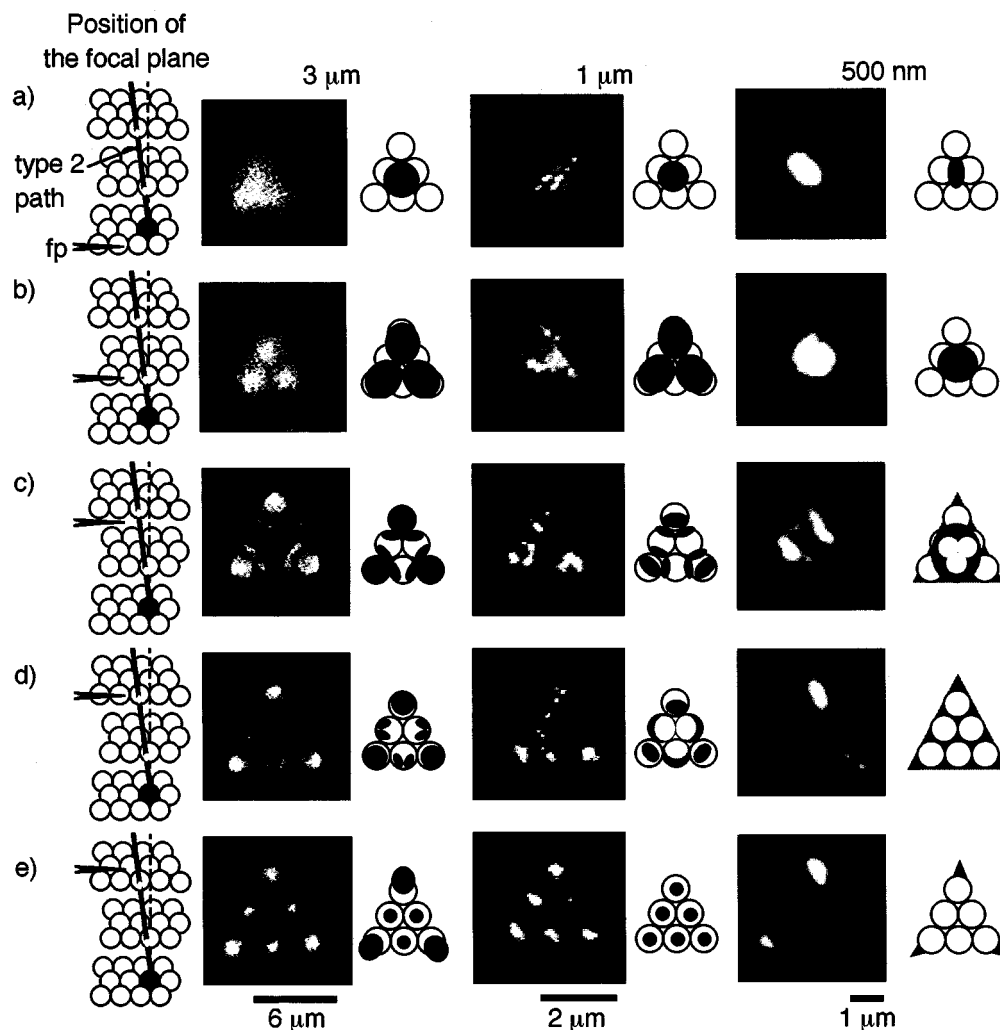


Figure 8. Detail depicting the light propagation patterns of cubic close-packed structure in a triple layer for particle diameters of 3, 1, and 0.5 μm . The fluorescent images are changed with the focal plane (fp) from the bottom layer (a) to the top layer (e). The schematic model is shown next to the fluorescent image.

of type 1 light. The same phenomenon can be observed in the monolayer as half-illuminated spots in the regions between the six bright lines (see Figure 5a,b). As the focal plane is raised to the middle of the third layer, each hat-shaped pattern divides into three parts, one large dot at each of the three vertexes of the triangle, due to particles that are on a direct straight line from the fluorescent particles, and two small oval-shaped dots on the sides of the triangle (Figure 8d). The propagation along the straight line is essentially type 2 propagation, as discussed above. Thus we designated this line as "type 2 path". Gradually the latter merge as the focal plane is raised. Finally, at the top of the layer, the two small ovals from each "hat" at the midpoint of each side of the triangle have completely merged, and we can observe a triangular pattern of six illuminated particles in the fcc domains (Figure 8e).

In the hcp domain, the pattern observed when the focal plane is at the bottom edge of the top layer has a flowerlike shape. This is composed of three small dots at the vertexes of a triangle (Figure 9c). Within the triangle, there are three small triangles each composed of three ovals. As the focus is raised to the middle of the top layer (Figure 9d), these small triangles take on a "wing" shape as the dots nearest the center become smaller and move toward the center. Simultaneously, the pairs of larger dots separate. These two dots are located on either side of the type 2 path, which is the same line that passes through the

centers of particles in all three layers in the fcc structure but passes between particles in the top layer in the hcp structure. In this case, the two particles on either side of the type 2 path form the wings. As the focus is raised to the top of the top layer (Figure 9e), the wings divide into two separate dots, and the small central dots merge and form a single central bright dot. At this point, we can observe a hexagon composed of seven illuminated particles.

The light propagation patterns in the 1 μm particle array are basically the same as those for the 3 μm array, but as shown in Figure 9c,d in the hcp domains, we cannot observe three small dots at the vertexes of a triangle, which we can observe in the 3 μm particle array. This difference might be related with the void sizes between the particles. For the case of the 3 μm particle array, the void size is submicrometer order, thus large enough to be passed through by the green light. On the other hand, inside of the 1 μm particle array, the void size is tens of nanometers. Therefore, we did not observe the three small dots in the 1 μm particle array.

In the case of the 500 nm diameter particles, the light propagation patterns were even more markedly different from those for the 3 μm particles. We can see typical differences in Figure 8e and 9e. The light is not exclusively centered on the tops of the particles but surrounds the perimeter of particles. An exception is observed for the center of the hcp pattern, which is positioned exactly above the fluorescent particle (Figure 9e, discussed later).

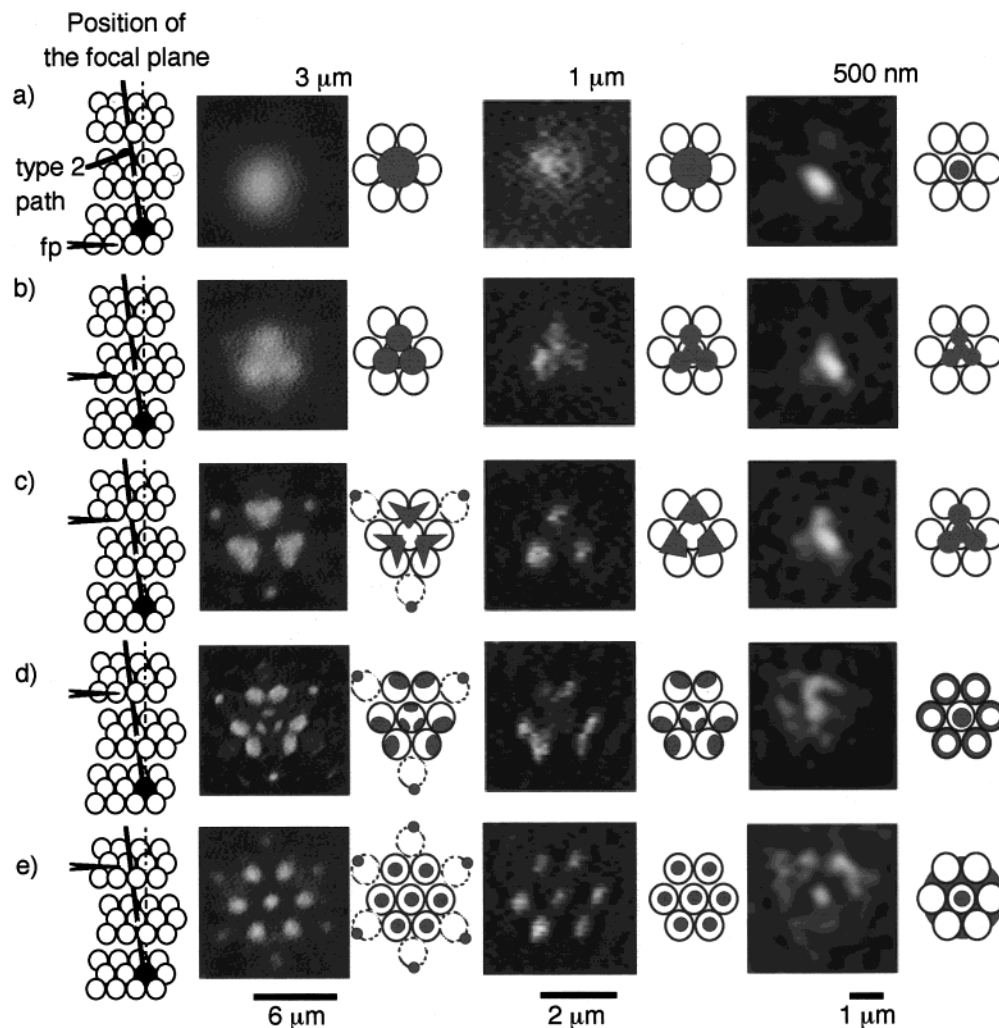


Figure 9. Detail depicting the light propagation patterns of hexagonal close-packed structure in a triple layer for particle diameters of 3, 1, and 0.5 μm . The fluorescence images show the focal plane (fp) shifting from the bottom layer (a) to the top layer (e). Corresponding schematic models are shown to the right of the fluorescence images.

The “surrounding” phenomena are consistent with the discussion of the type 4 propagation mode in connection with Figure 6. The particle size is of the same order of magnitude as the wavelength, so that the light cannot exist inside the sphere, and certainly not in the smaller voids between particles. Therefore, the contribution of the evanescent field is expected to increase. These images which were observed in the trilayer reinforce our hypothesis in the monolayer, that the evanescent field cannot be observed without a probe, and thus the adjoining particles should act as probes.

Regarding the center of the hcp pattern, we must consider the depth of focus of our objective lens, 0.37 μm . When the focal plane is in the middle of the top layer, the top of the bottom layer should also be in focus. Thus, we can observe the light dot on the center of the hcp pattern, which is positioned on the fluorescent particle.

Comparison with Theoretical Work. To establish the origins of the light propagation modes in this 2D array type of photonic device, further experimental and theoretical work needs to be carried out.^{33,34} A good example is the 1998 paper of Miyazaki and Ohtaka⁷ in which they calculated theoretical 2D electric field distributions based on photon multiple scattering theory, for light impinging on a single layer of close-packed spheres. Their calculations

suggest that the electromagnetic modes or field distribution patterns should depend on the particle size relative to the light wavelength. They define a relative light frequency ω to be $\sqrt{3}d/2\lambda$ in a hexagonal array, in which d is the lattice constant and λ is the wavelength. They found, as did Inoue et al. previously,³⁵ that there is a peak in the reflectivity at $\omega = 1.0$, above which the 6-fold symmetric propagation channels, one type of resonance, emanating from a given particle open.

Here we examine our experimental results in the light of these calculations. Considering the wavelength of green light (540 nm), ω takes the value 4.81 for the 3 μm diameter particle array, 1.60 for the 1 μm array, and 0.80 for the 0.5 μm array. Therefore, for the 3 and 1 μm diameter particle arrays, the channels can be open, but cannot be open for the 0.5 μm diameter particle array. Comparing with our fluorescent images, Figures 5, 6, 8, and 9, we propose that the type 2 propagation may be related to the opening of the channel. In other words, in the conditions which we can observe the type 2 propagation, such as the 3 and 1 μm diameter particle arrays, the light propagation channels are opened.

Soon it should be possible to reach a resonance condition with a type of 2D array similar to that reported here by properly matching the particle size and the fluorescence

(33) Ohtaka, K.; Tanabe, Y. *J. Phys. Soc. Jpn.* **1996**, *65*, 2265.

(34) Ohtaka, K.; Tanabe, Y. *J. Phys. Soc. Jpn.* **1996**, *65*, 2276.

(35) Inoue, M.; Ohtaka, K.; Yanagawa, S. *Phys. Rev. B* **1982**, *25*, 689.

emission wavelength. Work along these lines is in progress in our and other laboratories.³⁶ Thus, at present, we are only able to draw conclusions regarding the opening of the channel, without regard for the resonance conditions. To the best of our knowledge, this is the first report of the direct observation of the opening of light propagation channels.

Conclusion

We prepared a periodical dielectric structure, in the form of a two-dimensional array, in which fluorescent particles are involved as light sources, and examined how light propagates in the structure. The light propagation modes in two-dimensional spherical arrays can be mainly divided with two modes: one named straight-line propagation which propagates inside the particles and another is the scattering light of the evanescent field. The contributions of these two modes seem to be related with the relative light frequency $\omega = 1$,⁷ where ω is defined to be $\sqrt{3}d/2\lambda$ in the hexagonal array, in which d is the lattice constant and λ is the wavelength. We suggest that straight-line propagation means the opening of the 6-fold symmetric propagation channels. In future, if we control the value of ω , we will be able to have in situ observation of the opening of the photonic band. We believe that our

investigation of light propagation in ordered arrays of this type makes it possible to trace how the optical properties of photonic crystals evolve on going from two to three dimensions and from nonresonance to resonance light propagation conditions.

Moreover, our through-focusing observation makes it possible to directly determine the stacking mode of the two-dimensional spherical array. We believe that such information may help to expand the scope for basic research in the two-dimensional-array area. We hope that this approach could also be applied in the future to characterize the packing modes of other types of currently studied solid-state colloidal crystals (e.g., artificial opals and their replicas).

Acknowledgment. Thanks are due to Professor K. Hashimoto (Research Center for Advanced Science and Technology, University of Tokyo, Japan) for his valuable discussions and to Dr. A. S. Dimitrov (L'OREAL Tsukuba Center, Japan) for development of the glass cell used in the preparation of the particle coating. The present work has been partially supported by a Grant-in-Aid for Scientific Research from the Ministry of Education, Science, Sport and Culture of Japan, by the YKK R&D Center, and by the Circle for the Promotion of Science and Engineering.

(36) Kuwata-Gonokami, M.; Takeda, K.; Yasuda, H.; Ema, K. *Jpn. J. Appl. Phys.* **1992**, *31*, L99.